

Supporting Information

Luminescent 2-phenylbenzothiazole cyclometalated Pt^{II} and Ir^{III} complexes with chelating P^O ligands

David Gómez-de-Segura, Rebeca Lara, Mónica Martínez-Junquera, Elena Lalinde and M. Teresa Moreno*

Departamento de Química-Centro de Síntesis Química de La Rioja, (CISQ), Universidad de La Rioja, 26006, Logroño, Spain. E-mail: teresa.moreno@unirioja.es

Contents:	Page
1.- Characterization of Complexes.....	S2
1.1.- NMR Spectra.....	S2
1.2.- Crystal Structures	S9
2.- Photophysical Properties and Theoretical Calculations.....	S14

1.- Characterization of Complexes

1.1- NMR Spectra

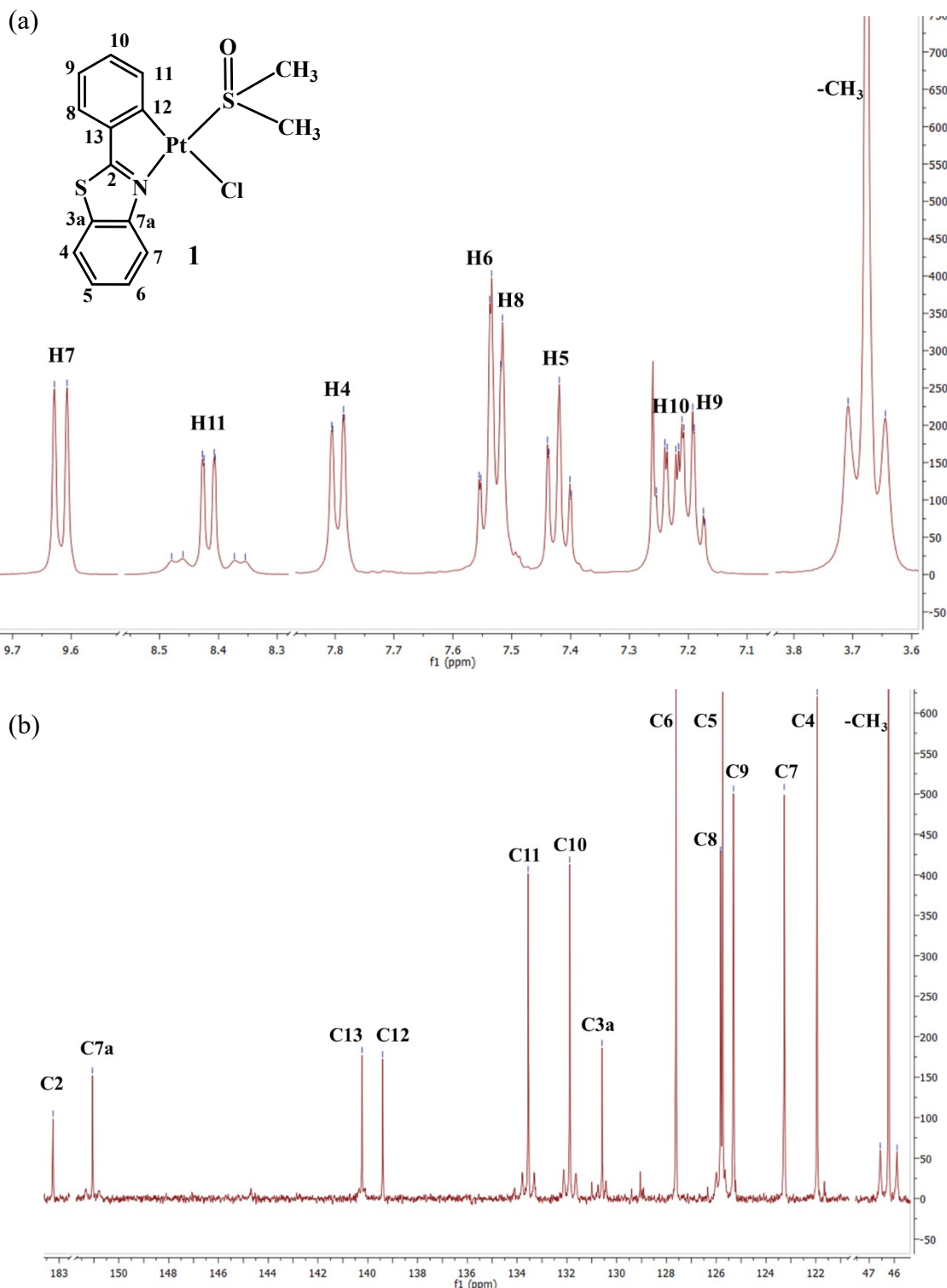


Fig. S1 NMR spectra of **1** in CDCl_3 at 298 K (a) ^1H , (b) $^{13}\text{C}\{^1\text{H}\}$

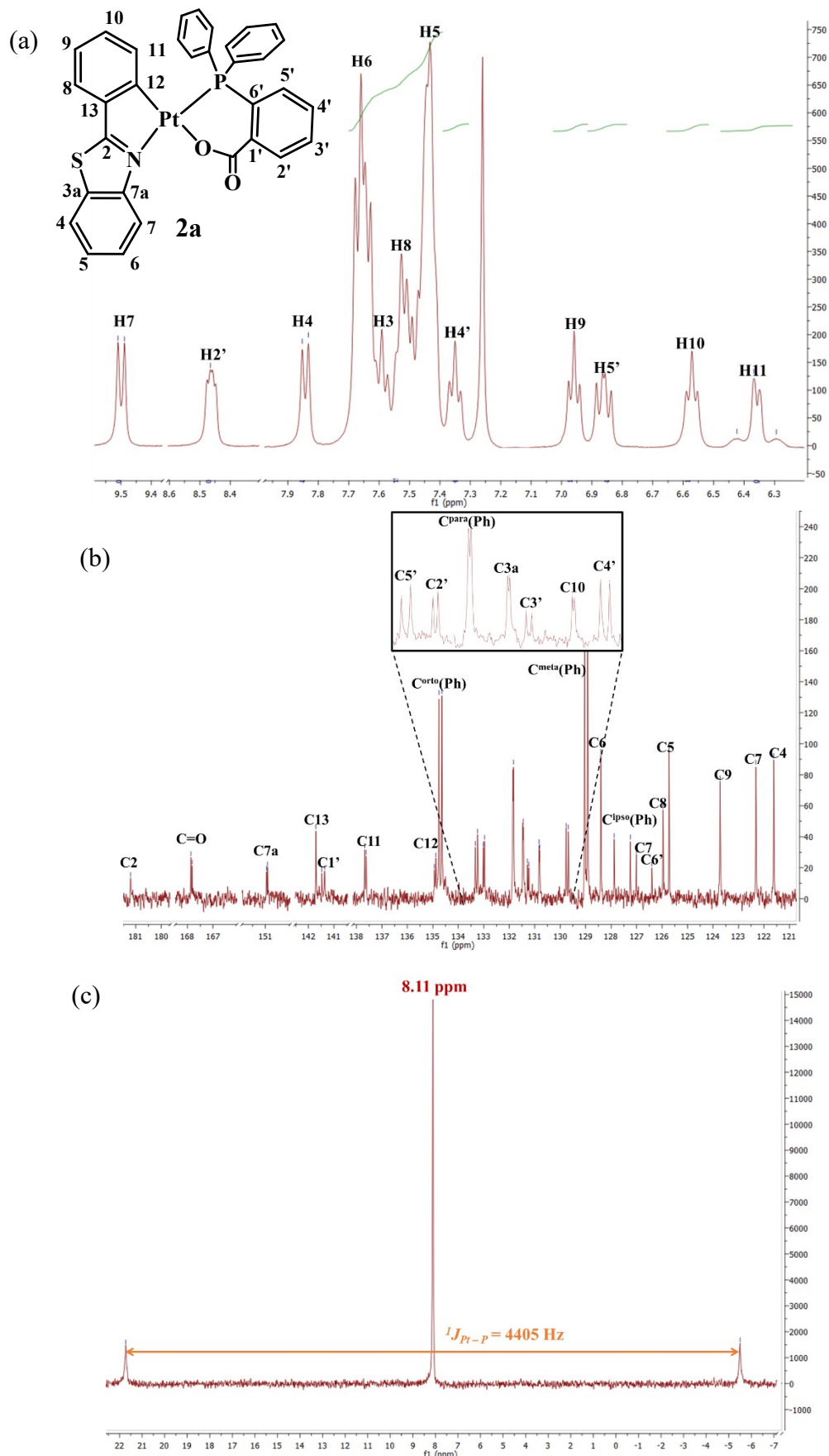


Fig. S2 NMR spectra of **2a** in CDCl_3 at 298 K (a) ^1H , (b) $^{13}\text{C}\{^1\text{H}\}$, (c) $^{31}\text{P}\{^1\text{H}\}$

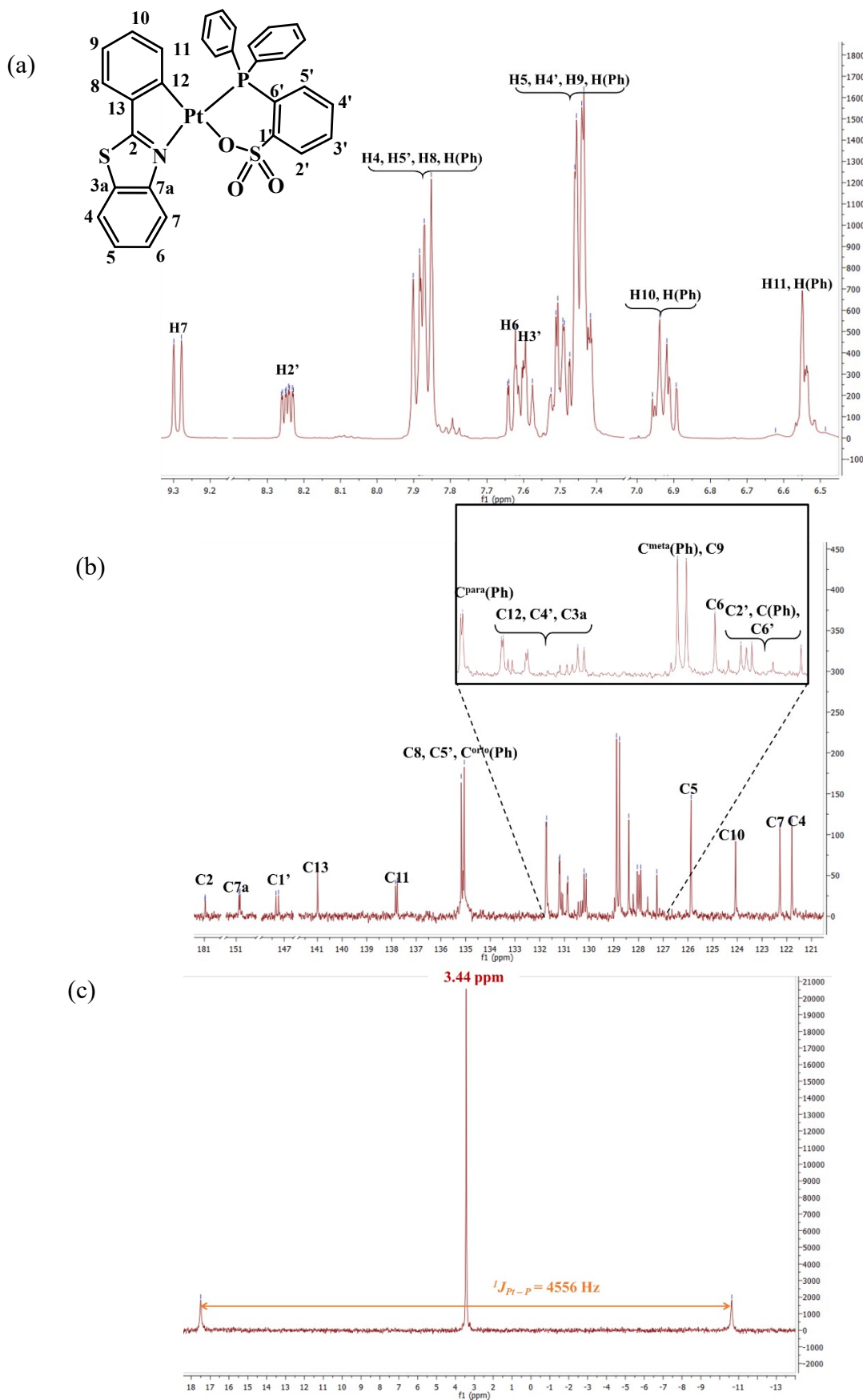


Fig. S3 NMR spectra of **2b** in CDCl_3 at 298 K (a) ^1H , (b) $^{13}\text{C}\{^1\text{H}\}$, (c) $^{31}\text{P}\{^1\text{H}\}$

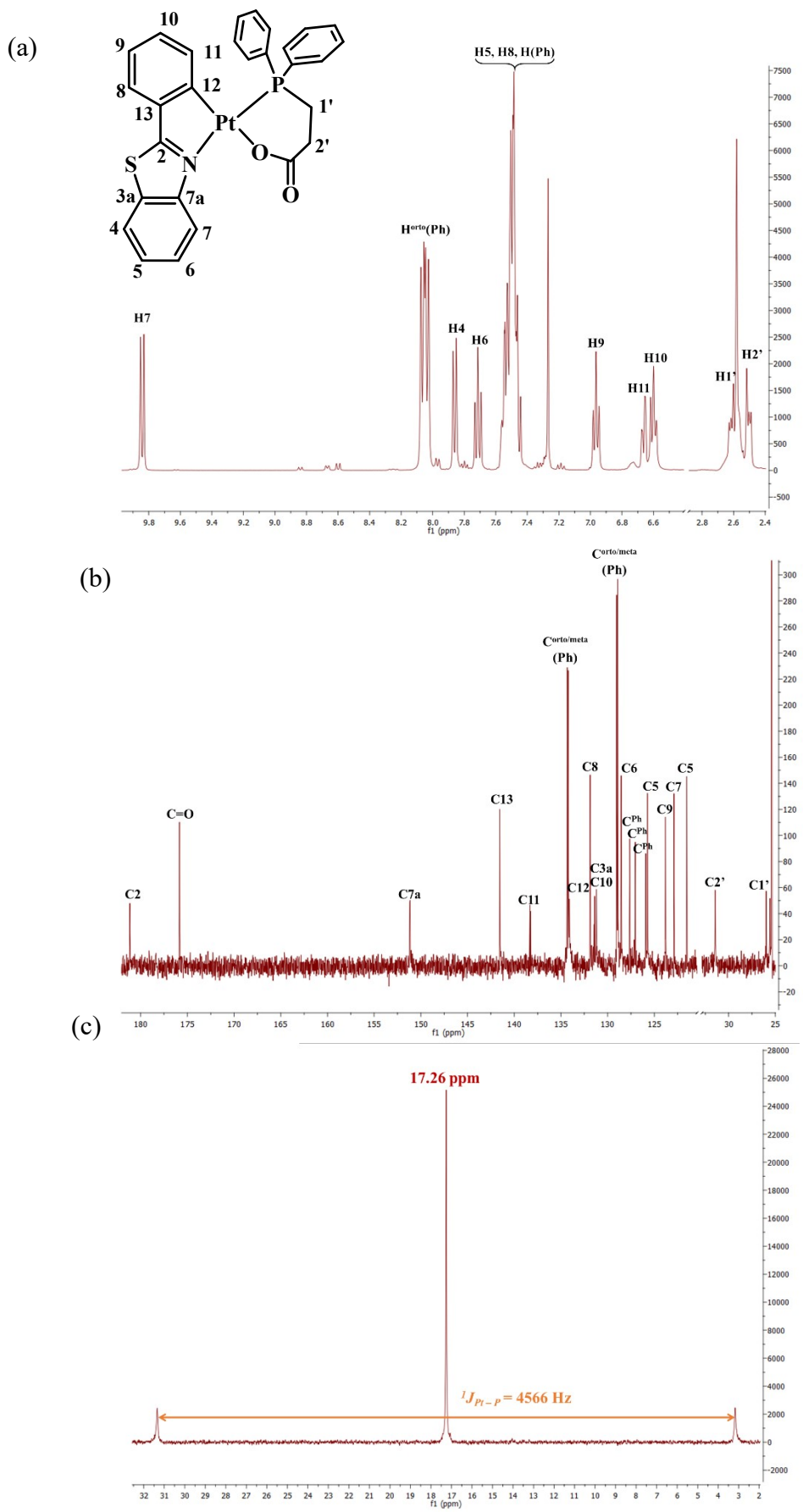


Fig. S4 NMR spectra of **2c** in CDCl_3 at 298 K (a) ^1H , (b) $^{13}\text{C}\{^1\text{H}\}$, (c) $^{31}\text{P}\{^1\text{H}\}$

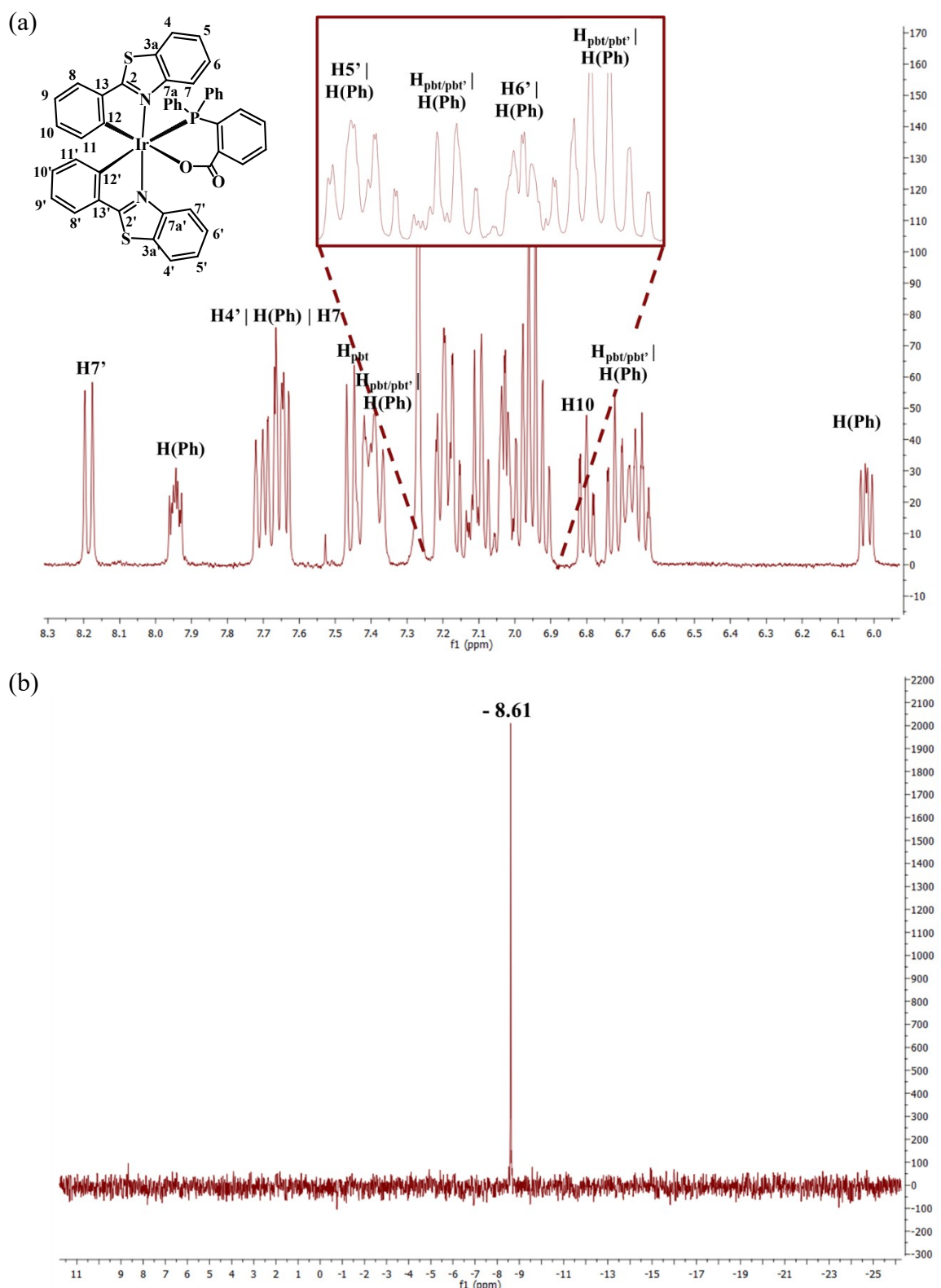


Fig. S5 NMR spectra of **3a** in CDCl_3 at 298 K (a) ^1H , (b) $^3\text{P}\{^1\text{H}\}$

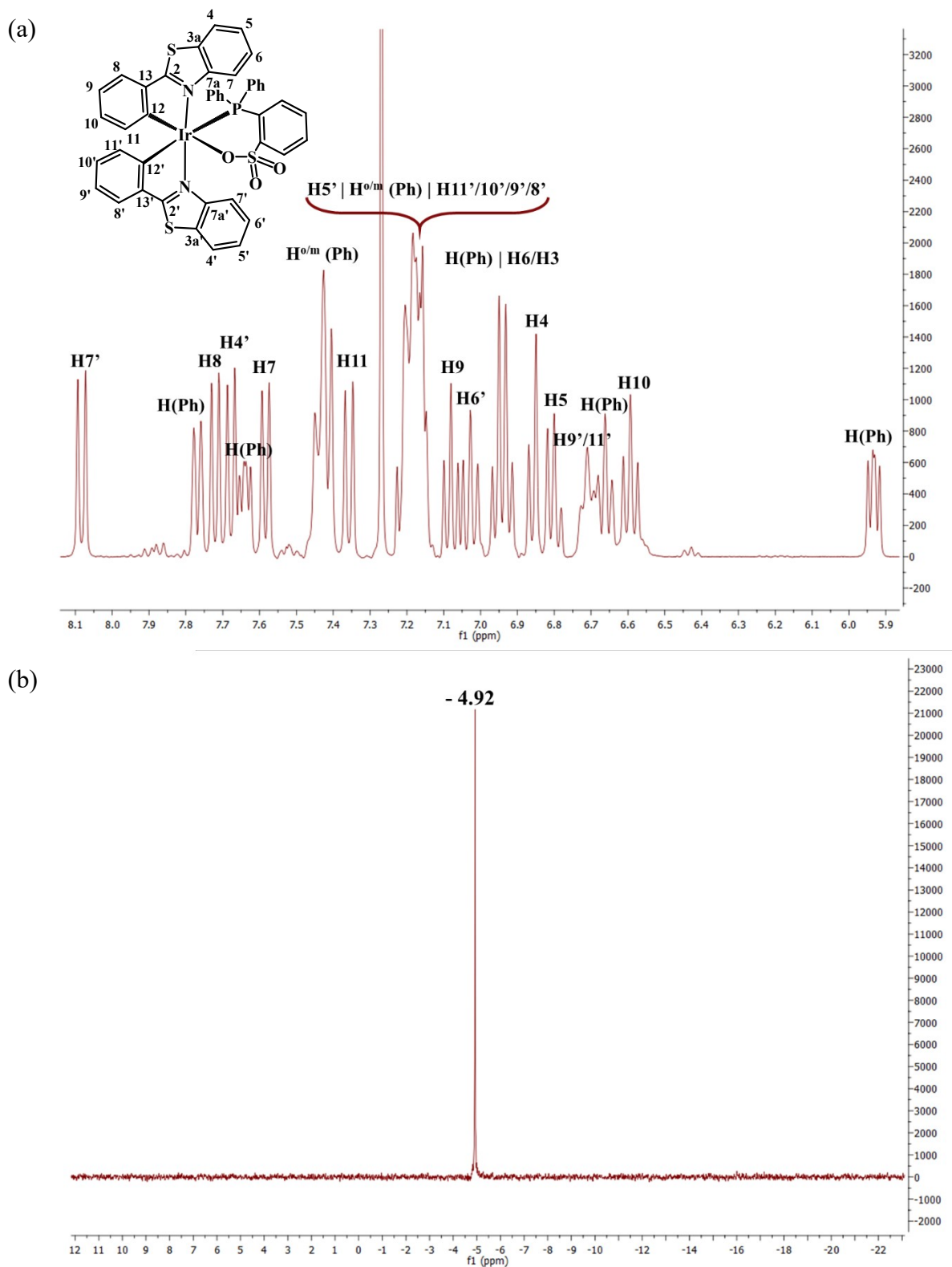


Fig. S6 NMR spectra of **3b** in CDCl_3 at 298 K (a) ^1H , (b) $^3\text{P}\{\text{H}\}$

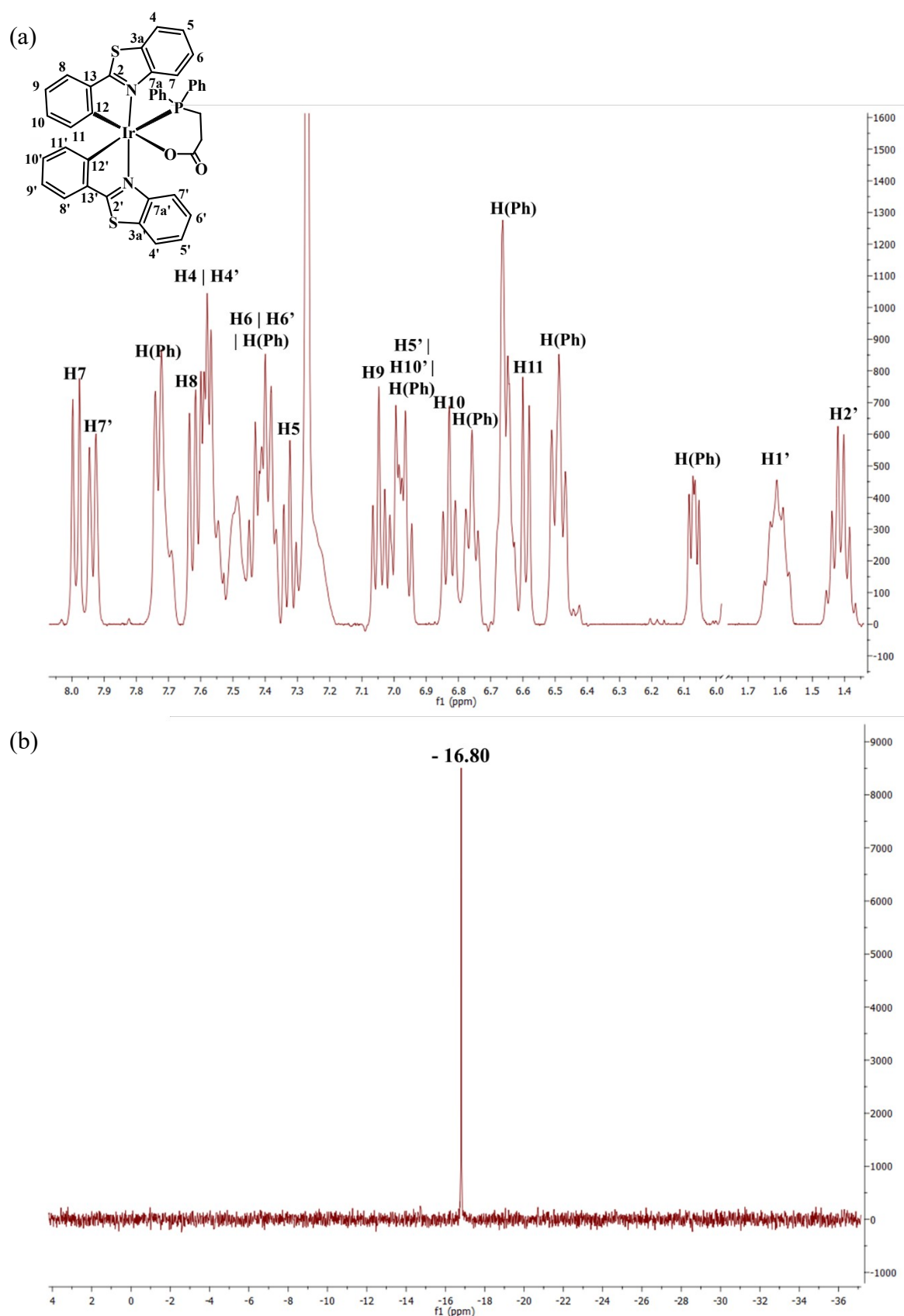


Fig. S7 NMR spectra of **3c** in CDCl_3 at 298 K (a) ^1H , (b) ${}^{31}\text{P}\{{}^1\text{H}\}$

1.2.- Crystal Structures

Table S1. X-ray crystallographic data for complexes **1**, **2a·H₂O** and **2b·0.5 CHCl₃**.

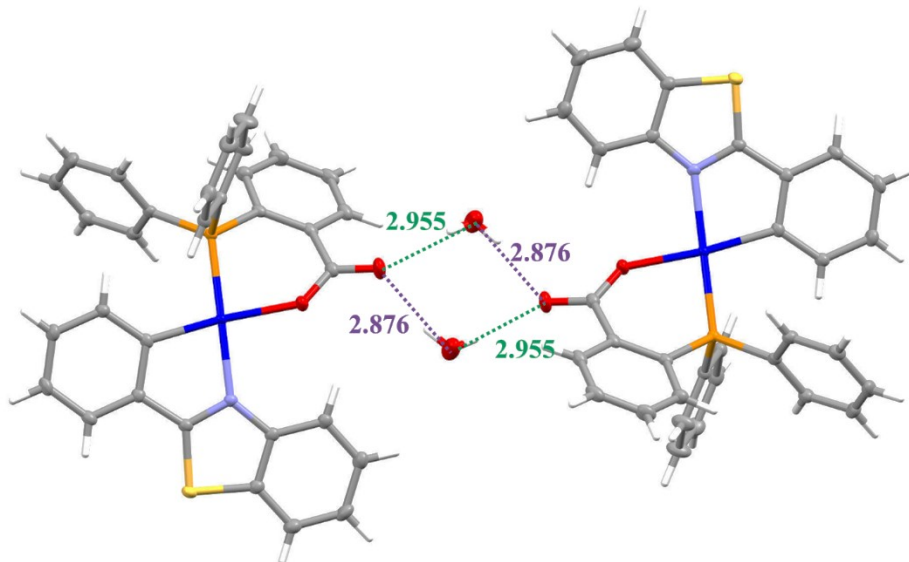
	1	2a·H₂O	2b·0.5 CHCl₃
Empirical formula	C ₁₅ H ₁₄ CINOPtS ₂	C ₃₂ H ₂₄ NO ₃ PPtS	C _{31.5} H _{22.5} Cl _{1.5} NO ₃ PPtS ₂
Molecular weight	518.93	728.63	806.36
T (K)	295(2)	145(1)	100(1)
Wavelength (Å)	0.71076	0.71076	0.71076
Crystal system	Orthorrombic	Triclinic	Monoclinic
Space group	P2 ₁ 2 ₁ 2 ₁	P-1	P 2 ₁ /n
Crystal size (mm)	0.324x0.232x0.166	0.220x0.160x0.158	0.183x0.163x0.070
a (Å)	5.9444(6)	9.5339(8)	9.4693(7)
b (Å)	10.8982(10)	11.7090(11)	21.7025(15)
c (Å)	24.027(2)	13.0973(12)	14.0447(10)
α (°)	90.0	82.876(3)	90.0
β (°)	90.0	72.589(3)	100.138(2)
γ (°)	90.0	71.732(3)	90.0
V (Å³)	1556.5(3)	1324.0(2)	2841.2(4)
Z	4	2	4
Density (calculated) (g/cm³)	2.214	1.828	1.885
Absorption coefficient (mm⁻¹)	9.451	5.474	5.319
F(000)	984	712	1572
θ range for data collection (°)	3.531 to 26.370	3.202 to 27.953	2.843 to 26.370
Index ranges	-7<=h<=7, -13<=k<=13, -30<=l<=30	-12<=h<=12, -15<=k<=15, -17<=l<=17	-11<=h<=11, -27<=k<=27, -17<=l<=17
Reflections collected	85598	77991	140753
Independent reflections	3185 [R(int) = 0.1219]	6346 [R(int) = 0.0433]	5801 [R(int) = 0.1179]
Data / restraints / parameters	3185 / 0 / 191	6346 / 0 / 360	5801 / 0 / 352
Goodness-of-fit on F²^[a]	1.236	1.161	1.073
Final R indices [I>2σ(I)]^[a]	R1 = 0.0196, wR2 = 0.0548	R1 = 0.0147, wR2 = 0.0361	R1 = 0.0304, wR2 = 0.0716
R indices (all data)^[a]	R1 = 0.0197, wR2 = 0.0548	R1 = 0.0164, wR2 = 0.0366	R1 = 0.0448, wR2 = 0.0793
Largest diff. peak and hole (e Å⁻³) (d_{min}/d_{max})	0.898 and -1.525	0.398 and -1.428	1.460 and -2.291

^[a] $R1 = \sum(|F_o| - |F_c|)/\sum|F_o|$; $wR2 = [\sum w(F_o^2 - F_c^2)^2/\sum wF_o^2]^{1/2}$; goodness of fit = $\{\sum[w(F_o^2 - F_c^2)^2]/(N_{obs} - N_{param})\}^{1/2}$; $w = [\sigma^2(F_o) + (g_1P)^2 + g_2P]^{-1}$; $P = [\max(F_o^2; 0 + 2F_c^2)]/3$.

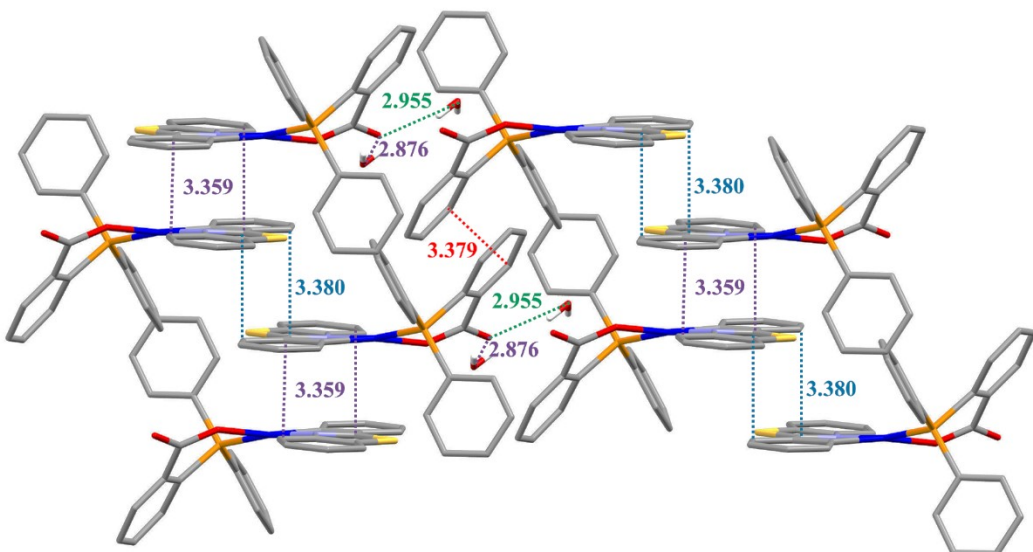
Table S2. X-ray crystallographic data for complexes **2c**·THF, **3a**·2.75CHCl₃ and **3b**·1.5CH₃COCH₃.

	2c ·THF	3a ·2.75CHCl ₃	3b ·1.5CH ₃ COCH ₃
Empirical formula	C ₃₂ H ₃₀ NO ₃ PPtS	C _{47.75} H _{32.75} Cl _{8.25} IrN ₂ O ₂ PS ₂	C _{48.5} H ₃₉ IrN ₂ O _{4.5} PS ₃
Molecular weight	734.69	1246.26	1041.16
T (K)	120(1)	173 (2)	100(1)
Wavelength (Å)	0.71076	0.71076	0.71076
Crystal system	Monoclinic	Monoclinic	Monoclinic
Space group	C c	P 2 ₁ /c	P 2 ₁ /n
Crystal size (mm)	0.294 x 0.190 x 0.149	0.150 x 0.120 x 0.100	0.277 x 0.149 x 0.133
a (Å)	9.0583(12)	18.8070(5)	12.210(3)
b (Å)	29.188(4)	14.4455(5)	18.957(5)
c (Å)	10.3424(14)	19.5948(5)	18.462(6)
α (°)	90	90	90
β (°)	91.914(4)	117.317(2)	96.050(12)
γ (°)	90	90	90
V (Å³)	2732.9(6)	4729.8(3)	4249(2)
Z	4	4	4
Density (calculated) (g/cm³)	1.786	1.750	1.627
Absorption coefficient (mm⁻¹)	5.305	3.454	3.377
F(000)	1448	2454	2080
θ range for data collection (°)	3.074 to 27.940	2.516 to 25.681	2.848 to 27.918
Index ranges	-11<=h<=11, -38<=k<=38, -13<=l<=13	-22<=h<=22, -17<=k<=17, -23<=l<=23	-16<=h<=16, -24<=k<=24, -24<=l<=24
Reflections collected	85642	34520	99536
Independent reflections	6418 [R(int) = 0.0265]	8879 [R(int) = 0.0664]	10160 [R(int) = 0.0218]
Data / restraints / parameters	6418 / 2 / 353	8879 / 0 / 550	10160 / 0 / 524
Goodness-of-fit on F²[^a]	1.074	1.037	1.075
Final R indices [I>2σ(I)]^[a]	R1 = 0.0155, wR2 = 0.0403	R1 = 0.0397, wR2 = 0.0935	R1 = 0.0170, wR2 = 0.0405
R indices (all data)^[a]	R1 = 0.0157, wR2 = 0.0404	R1 = 0.0550, wR2 = 0.1009	R1 = 0.0190, wR2 = 0.0421
Largest diff. peak and hole (e Å⁻³) (d_{min}/d_{max})	1.125 and -0.961	1.353 and -1.501	0.618 and -0.910

^[a] $R1 = \sum(|F_o| - |F_c|)/\sum|F_o|$; $wR2 = [\sum w(F_o^2 - F_c^2)^2/\sum wF_o^2]^{1/2}$; goodness of fit = $\{\sum[w(F_o^2 - F_c^2)^2]/(N_{obs} - N_{param})\}^{1/2}$; $w = [\sigma^2(F_o) + (g_1P)^2 + g_2P]^{-1}$; $P = [\max(F_o^2; 0 + 2F_c^2)]/3$.



a)



b)

Fig. S8 a) Hydrogen bonds between two molecules of **2a** through the H_2O crystallization molecules (2.876 and 2.955 Å) and b) crystal packing of **2a** ($\pi \cdots \pi$ interactions: 3.359, 3.380 and 3.379 Å).

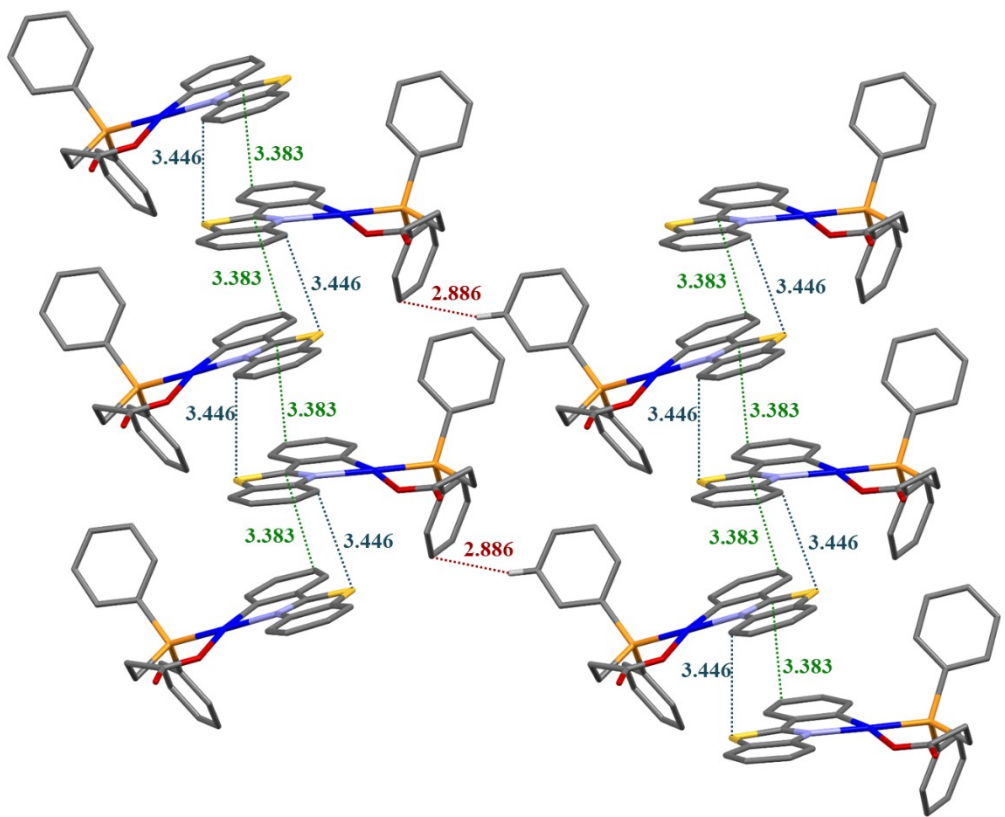


Fig. S9 Crystal packing of **2c** showing a head-to-head columnar stacking through $\pi\cdots\pi$ interactions (3.383 and 3.446 Å) attached by $S\cdots H$ and $C-H\cdots\pi$ interactions (red dots 2.886 Å).

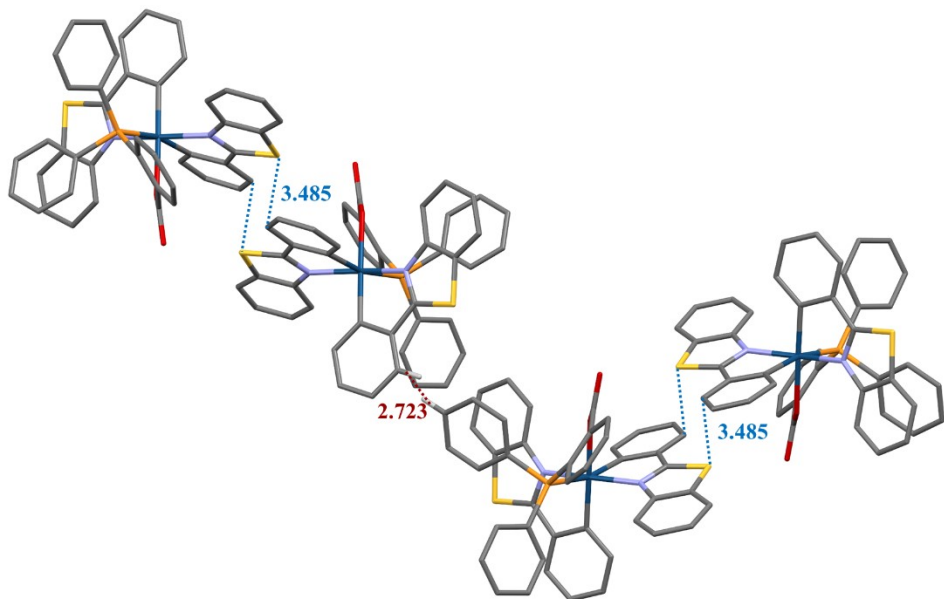


Fig. S10 Crystal packing of **3a** showing dimers connected by S···C-H interactions (3.485 Å) and attached by C-H···π interactions (2.723 Å) between the aryl of the phosphines.

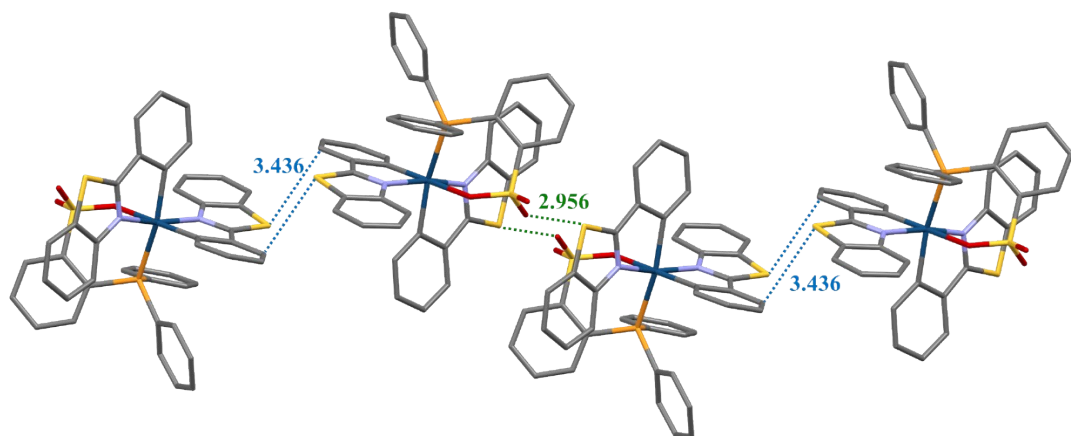


Fig. S11 Crystal packing of **3b** showing dimers connected by S···C-H interactions (3.436 Å) and attached by S···O interactions (2.956 Å).

2.- Photophysical Properties and Theoretical Calculations

Compound	$\lambda_{\text{abs}}/\text{nm}$ ($\varepsilon \times 10^{-3}/\text{M}^{-1}\text{cm}^{-1}$)
[Pt(pbt)Cl(DMSO)] 1	231 (25.97), 256 (20.91), 321 (16.75), 335 (16.45), 389 (5.90), 407 (4.77)
[Pt(pbt){PPh ₂ (<i>o</i> -C ₆ H ₄ COO)-κ <i>P,O</i> }] 2a	235 (45.2), 258 (23.54), 320 (18.32), 334 (16.71), 395 (5.91), 414 (5.12)
[Pt(pbt){PPh ₂ (<i>o</i> -C ₆ H ₄ SO ₃)-κ <i>P,O</i> }] 2b	232 (43.43), 260 (21.06), 266 (19.86), 319 (16.25), 334 (15.85), 387 (6.42), 407 (5.03)
[Pt(pbt){PPh ₂ (CH ₂ CH ₂ CO ₂)-κ <i>P,O</i> }] 2c	230 (25.98), 261 (13.20), 268 (14.30), 280 _h (10.81), 320 (11.50), 333 (11.0), 393 (3.65), 412 (3.10)
[Ir(pbt) ₂ {PPh ₂ (<i>o</i> -C ₆ H ₄ CO ₂)-κ <i>PO</i> }] 3a	235 (65.6), 240 (51.3), 248 (43.1), 258 _h (36.4), 312 _{sh} (23.0), 323 (25.3), 346 _{sh} (12.7), 380 (7.2), 425 (6.8), 448 (4.9)
[Ir(pbt) ₂ {PPh ₂ (<i>o</i> -C ₆ H ₄ SO ₃)-κ <i>PO</i> }] 3b	233 (62.7), 249 _{sh} (44.7), 279 _{sh} (26.7), 313 _{sh} (27.7), 323 (30.4), 375 (8.5), 417 (7.8), 441 (5.2)
[Ir(pbt) ₂ {PPh ₂ (CH ₂ CH ₂ CO ₂)-κ <i>PO</i> }] 3c	233 (34.3), 258 _{sh} (18.2), 311 (15.5), 322 (17.4), 377 (4.4), 406 (4.3), 429 (3.3)

Table S4. DFT optimized geometries for ground state and triplet state (in CH₂Cl₂) for **1**, **2a**, **2b**, **2c** and **3a**.

	1		
	X-ray	S ₀	T ₁
Pt(1) - C(1)	2.031(7)	2.02664	2.00597
Pt(1) - N(1)	2.087(6)	2.11333	2.06379
Pt(1) - S(2)	2.2201(17)	2.33572	2.36350
Pt(1) - Cl(1)	2.3851(19)	2.54382	2.55149
C(1)-Pt(1)-N(1)	80.4(3)	80.24179	81.53280
N(1)-Pt(1)-Cl(1)	93.89(17)	97.80613	96.88093
Cl(1)-Pt(1)-S(2)	87.63(7)	84.67648	84.23069
S(2)-Pt(1)-C(1)	97.2(2)	97.76147	97.62065
	2a		
	X-ray	S ₀	T ₁
Pt(1) - N(1)	2.1058(15)	2.15416	2.10705
Pt(1) - P(1)	2.2073(5)	2.27194	2.29072
Pt(1) - C(1)	2.0074(19)	2.01983	1.99307
Pt(1) - O(1)	2.1071(14)	2.14871	2.15922
C(1)-Pt(1)-N(1)	80.59(7)	79.87459	81.39307
P(1)-Pt(1)-O(1)	86.03(4)	82.11212	81.03841
C(1)-Pt(1)-P(1)	100.03(6)	100.94389	103.79424
O(1)-Pt(1)-N(1)	94.36(6)	94.65041	94.39409
	2b		
	X-ray	S ₀	T ₁
Pt(1) - C(1)	2.001(5)	2.01993	1.99575
Pt(1) - N(1)	2.100(3)	2.15360	2.10942
Pt(1) - O(1)	2.140(3)	2.19704	2.19942
Pt(1) - P(1)	2.2286(11)	2.30235	2.32291
C(1)-Pt(1)-N(1)	81.19(16)	80.31246	81.86451
N(1)-Pt(1)-O(1)	90.53(13)	91.77995	91.18401
O(1)-Pt(1)-P(1)	91.29(9)	90.14244	89.50541
P(1)-Pt(1)-C(1)	97.39(13)	97.80250	97.51585
	2c		
	X-ray	S ₀	T ₁
Pt(1)-C(1)	2.002(4)	2.01891	1.99220
Pt(1)-O(1)	2.090(3)	2.15668	2.16105
Pt(1)-N(1)	2.115(3)	2.16521	2.11988
Pt(1)-P(1)	2.2028(9)	2.27166	2.29074
C(1)-Pt(1)-N(1)	81.26(15)	80.25545	81.88908
O(1)-Pt(1)-N(1)	90.13(13)	91.48986	90.73013
C(1)-Pt(1)-P(1)	96.13(12)	98.54182	98.31041
O(1)-Pt(1)-P(1)	92.48(8)	89.71482	89.06868

3a

	X-ray	S ₀	T ₁
Ir(1)-C(13)	1.996(5)	2.01348	2.01905
Ir(1)-C(26)	2.055(5)	2.04818	2.03723
Ir(1)-P(1)	2.3884(14)	2.48790	2.50844
Ir(1)-O(2)	2.240(3)	2.22488	2.22228
Ir(1)-N(1)	2.065(4)	2.09095	2.10966
Ir(1)-N(2)	2.093(4)	2.12516	2.05118
C(45)-O(1)	1.318(6)	1.23806	1.23715
C(45)-O(2)	1.235(6)	1.29330	1.29427
C(13)-Ir(1)-P(1)	98.96(15)	104.10542	103.97608
C(13)-Ir(1)-C(26)	93.7(2)	92.79224	92.27038
C(13)-Ir(1)-N(1)	80.35(19)	79.79842	79.62151
C(13)-Ir(1)-N(2)	95.33(19)	95.10615	95.64981
C(26)-Ir(1)-O(2)	88.50(17)	88.06409	88.57991
C(26)-Ir(1)-N(1)	89.94(18)	91.08715	91.27885
C(26)-Ir(1)-N(2)	79.62(18)	79.16154	80.81114
N(1)-Ir(1)-O(2)	100.01(15)	96.16960	95.77632
N(1)-Ir(1)-P(1)	88.70(12)	90.42054	90.02680
N(2)-Ir(1)-O(2)	84.72(1)	89.0040	89.01463
N(2)-Ir(1)-P(1)	102.58(12)	100.50186	98.95958
O(2)-Ir(1)-P(1)	78.90(10)	74.97205	75.09070

			HOMO->L+1 (56%)
T ₂	492,56761	-	H-1->LUMO (41%), HOMO->LUMO (33%), HOMO->L+1 (12%)
T ₃	442,895596	-	H-1->LUMO (32%), HOMO->LUMO (41%)
S ₁	435,36833	0,0973	HOMO->LUMO (92%)
S ₂	425,828386	0,026	HOMO->L+1 (93%)
S ₃	368,978611	0,0065	H-1->LUMO (13%), H-1->L+1 (73%)
S ₄	367,447671	0,078	H-1->LUMO (77%), H-1->L+1 (13%)
S ₅	347,401701	0,0014	H-2->LUMO (84%)
S ₆	340,382136	0,0014	HOMO->L+2 (88%)
S ₇	336,849493	0,0266	H-3->LUMO (80%)

Table S6. Composition (%) of Frontier MOs in terms of ligands and metals in the ground state in CH₂Cl₂ for **1**, **2a**, **2b**, **2c** and **3a**.

1					
MO	eV	Pt	pbt	DMSO	Cl
LUMO+5	0.03	1	99	1	0
LUMO+4	-0.07	6	90	4	0
LUMO+3	-0.43	2	97	1	0
LUMO+2	-0.51	25	67	7	1
LUMO+1	-1.36	47	31	17	5
LUMO	-2.15	6	93	1	0
HOMO	-6.03	27	65	0	7
HOMO-1	-6.47	22	68	1	10
HOMO-2	-6.64	74	23	3	1
HOMO-3	-6.68	18	78	1	3
HOMO-4	-7.03	15	12	4	69
HOMO-5	-7.33	10	42	2	46
2a					
MO	eV	Pt	pbt	P^O	
LUMO+5	-0,49	10	19	70	
LUMO+4	-0,74	8	5	88	
LUMO+3	-0,96	1	1	98	
LUMO+2	-1,09	7	6	87	
LUMO+1	-1,4	10	9	81	
LUMO	-2	5	91	4	
HOMO	-5,87	31	63	6	
HOMO-1	-6,33	44	41	15	
HOMO-2	-6,39	53	32	15	
HOMO-3	-6,57	9	75	16	
HOMO-4	-6,64	4	29	66	
HOMO-5	-6,81	24	7	69	
2b					
MO	eV	Pt	pbt	P^O	
LUMO+5	-0,56	11	28	61	
LUMO+4	-0,8	5	3	92	
LUMO+3	-1,08	6	3	91	
LUMO+2	-1,15	12	10	77	
LUMO+1	-1,38	10	8	82	
LUMO	-2,08	5	92	3	
HOMO	-6,01	28	69	3	
HOMO-1	-6,47	84	4	12	
HOMO-2	-6,5	19	76	4	
HOMO-3	-6,64	8	91	1	
HOMO-4	-7,04	7	6	87	
HOMO-5	-7,12	1	1	98	

2c

MO	eV	Pt	pbt	P^O
LUMO+5	-0,33	7	76	17
LUMO+4	-0,51	4	7	89
LUMO+3	-0,59	15	26	58
LUMO+2	-0,96	11	8	81
LUMO+1	-1,11	6	5	89
LUMO	-1,99	5	93	2
HOMO	-5,83	32	55	13
HOMO-1	-6,3	6	40	53
HOMO-2	-6,41	13	34	53
HOMO-3	-6,43	87	6	7
HOMO-4	-6,57	6	92	1
HOMO-5	-6,74	20	20	59

3a

MO	eV	Ir	pbt(1)	pbt(2)	P^O
LUMO+5	-0,52	2	3	21	75
LUMO+4	-0,68	4	4	9	84
LUMO+3	-0,81	3	3	2	92
LUMO+2	-1,18	3	1	5	92
LUMO+1	-1,86	3	90	5	2
LUMO	-1,9	3	5	91	2
HOMO	-5,46	38	35	19	8
HOMO-1	-5,93	30	17	44	9
HOMO-2	-6,12	19	52	10	20
HOMO-3	-6,26	9	15	20	56
HOMO-4	-6,4	15	7	56	23
HOMO-5	-6,45	20	53	16	11

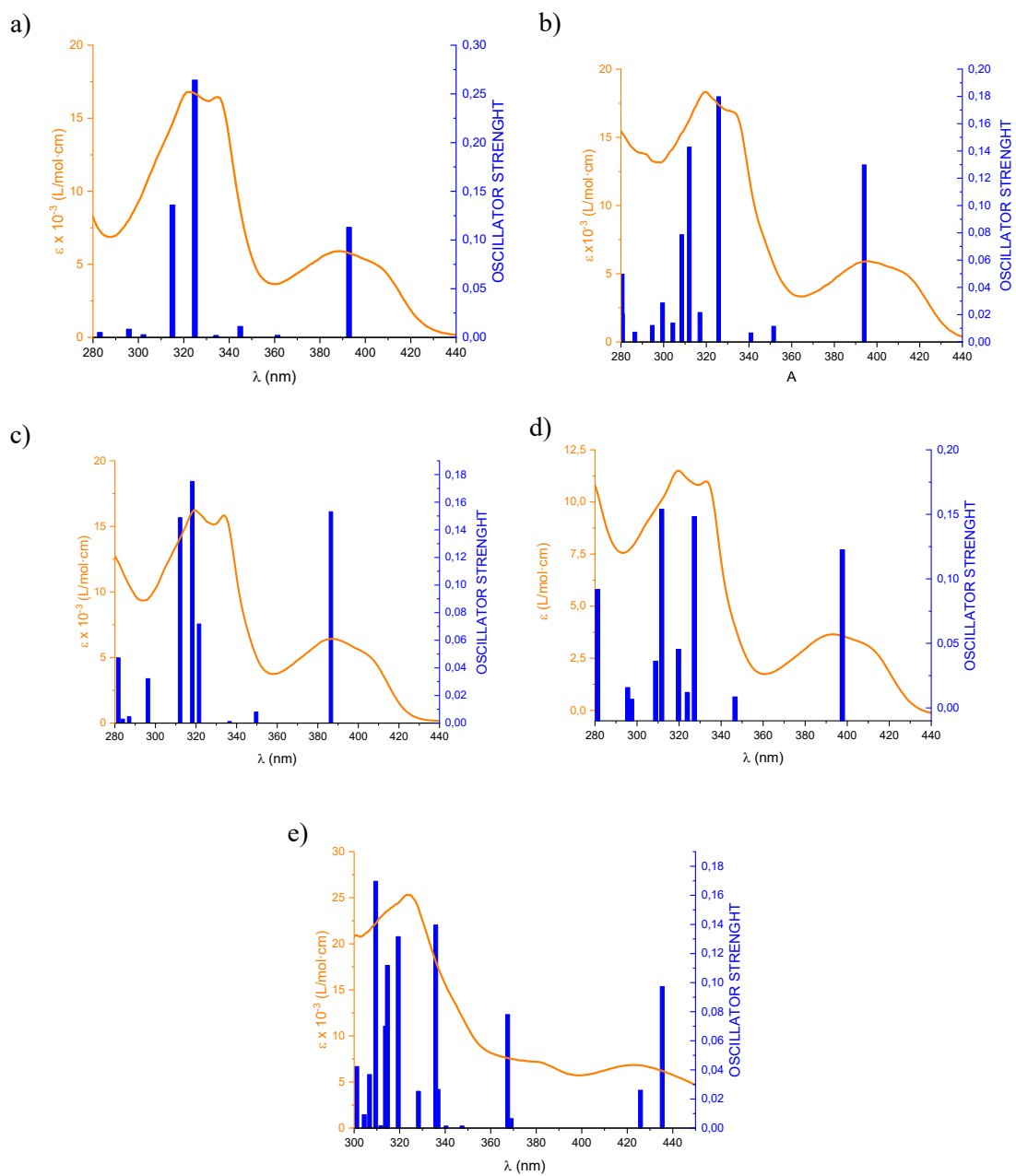
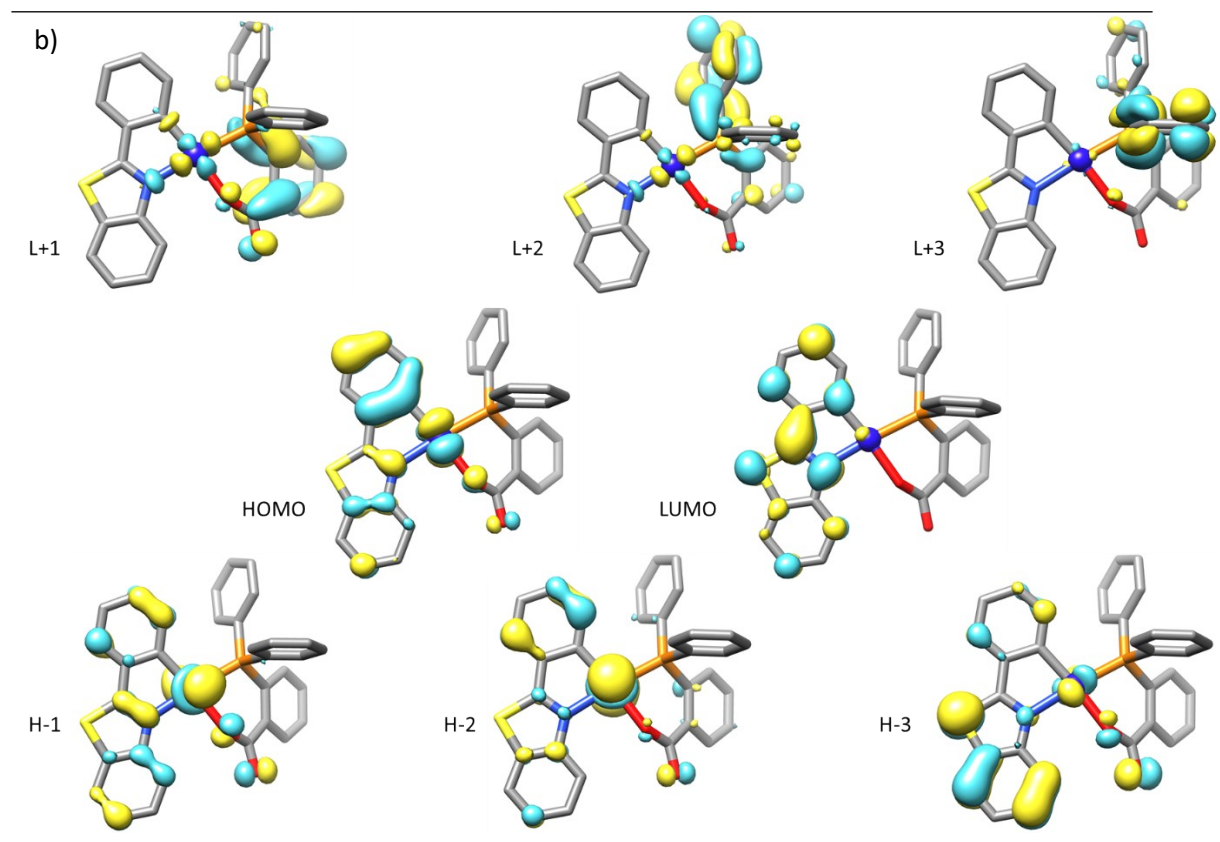
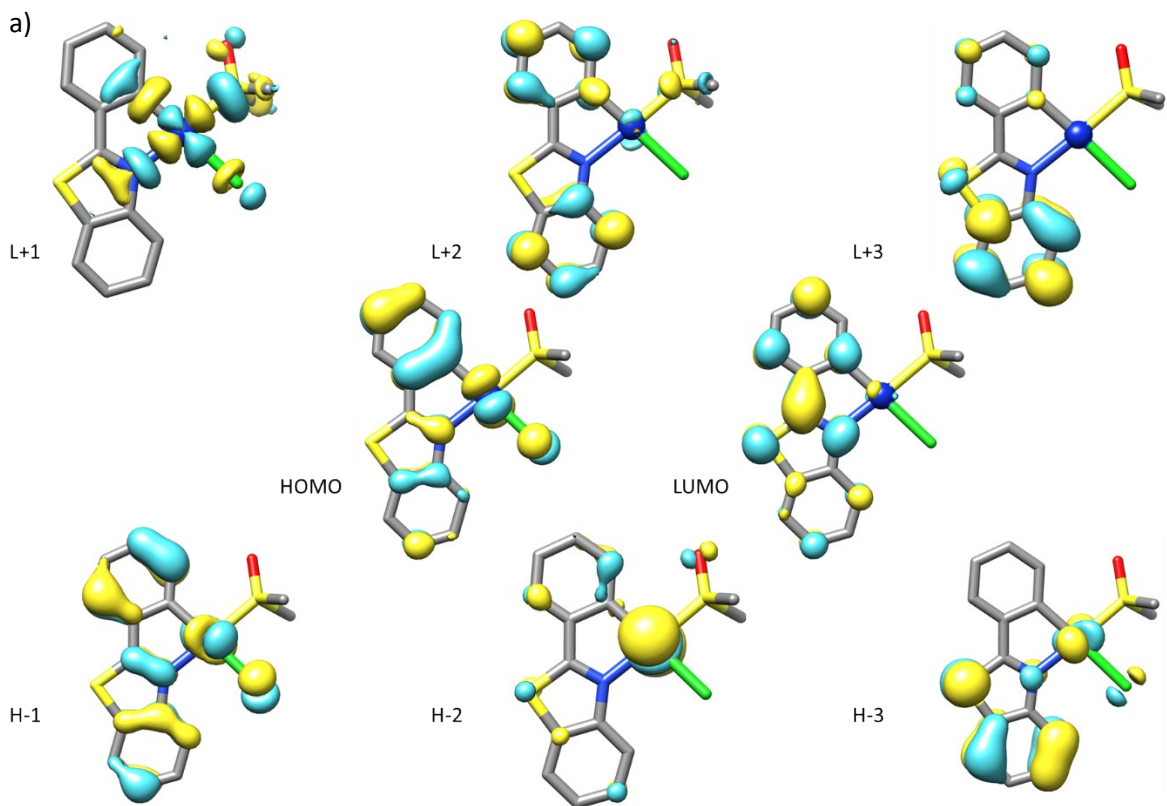
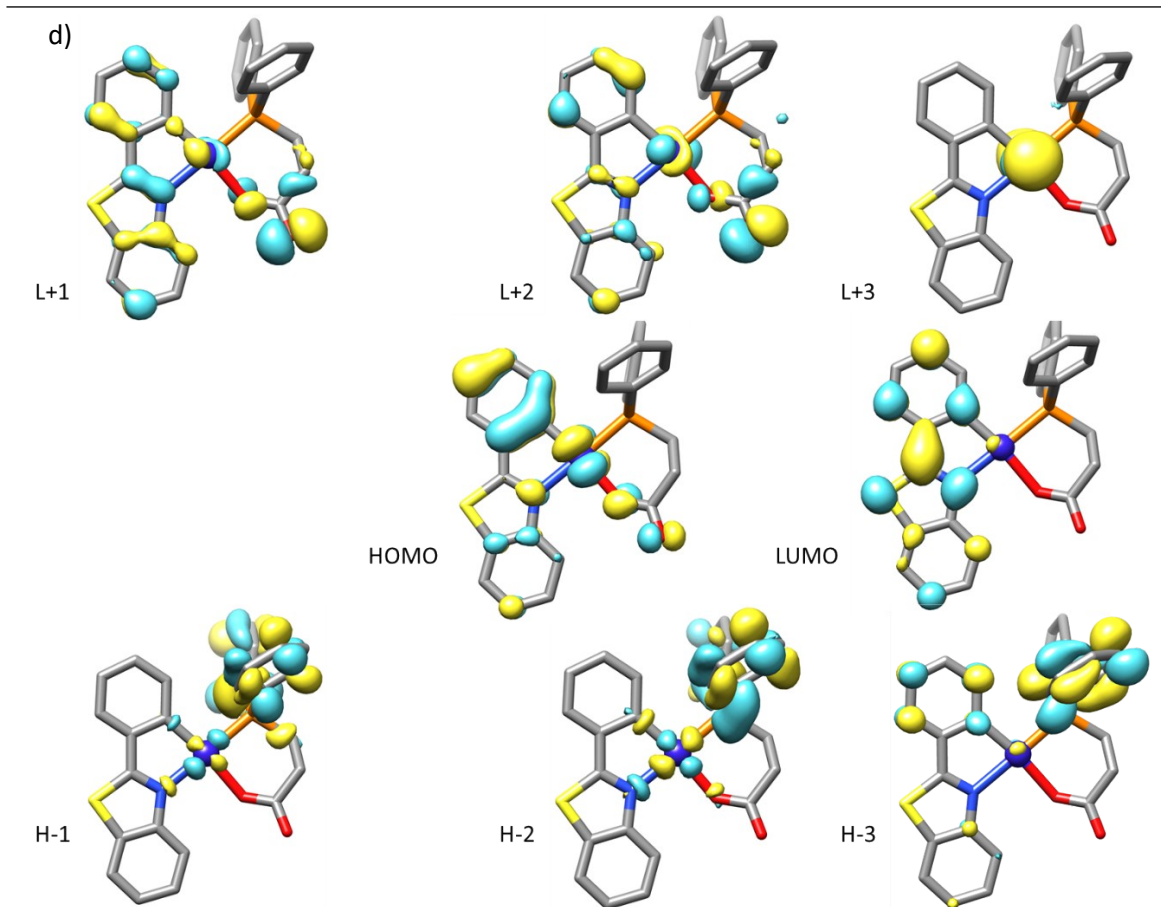
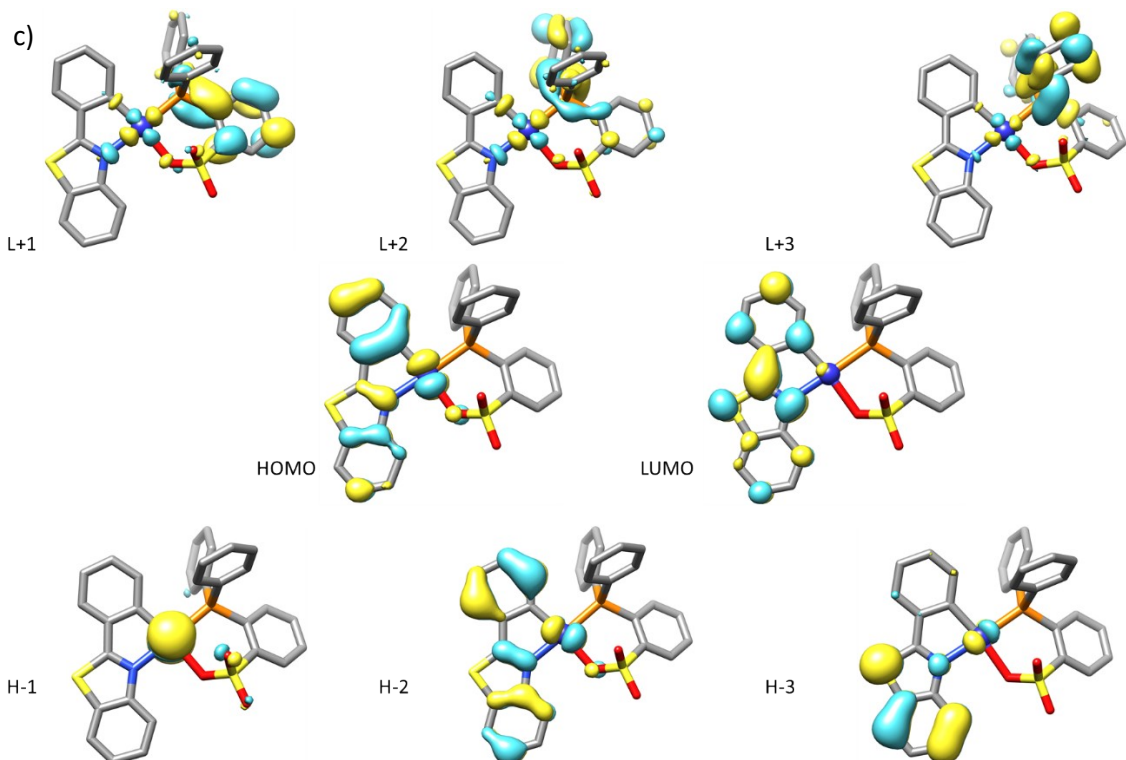


Fig. S12 Calculated stick absorption spectra of a) **1**, b) **2a**, c) **2b**, d) **2c** and d) **3a** in CH_2Cl_2 compared with the experimental spectra.





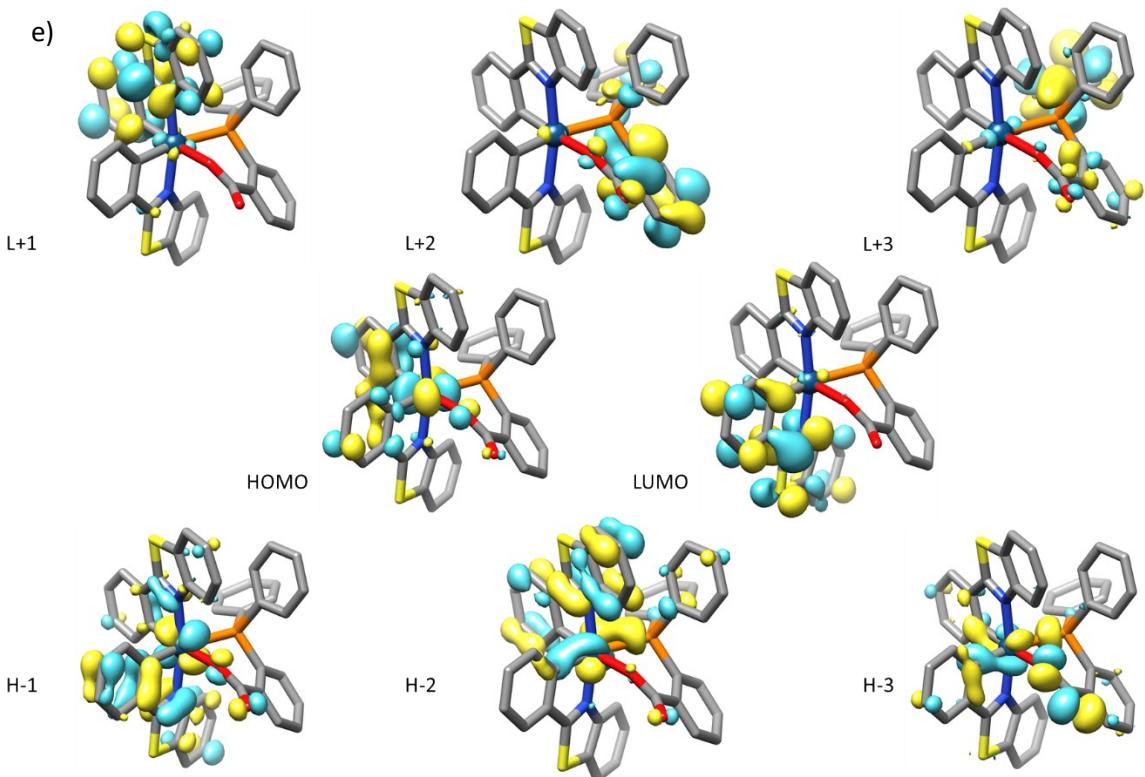


Fig. S13 Selected frontier Molecular Orbitals for a) **1**, b) **2a**, c) **2b**, d) **2c** and d) **3a** in the ground state.

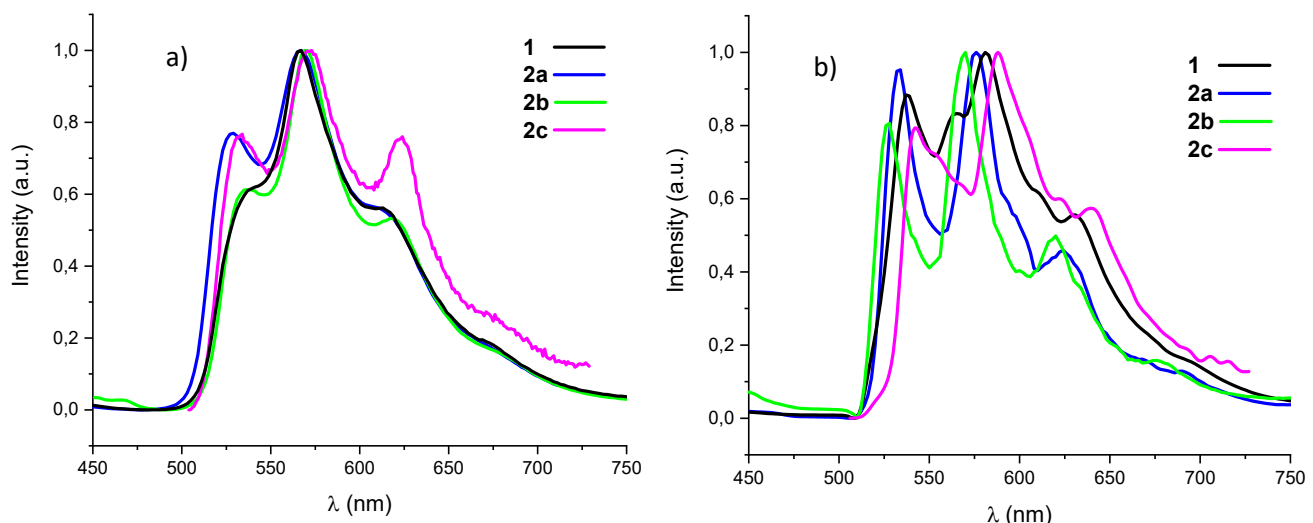


Fig. S14 Emission spectra of platinum complexes in solid state a) at 298 K, b) 77 K (λ_{exc} 400-420 nm).

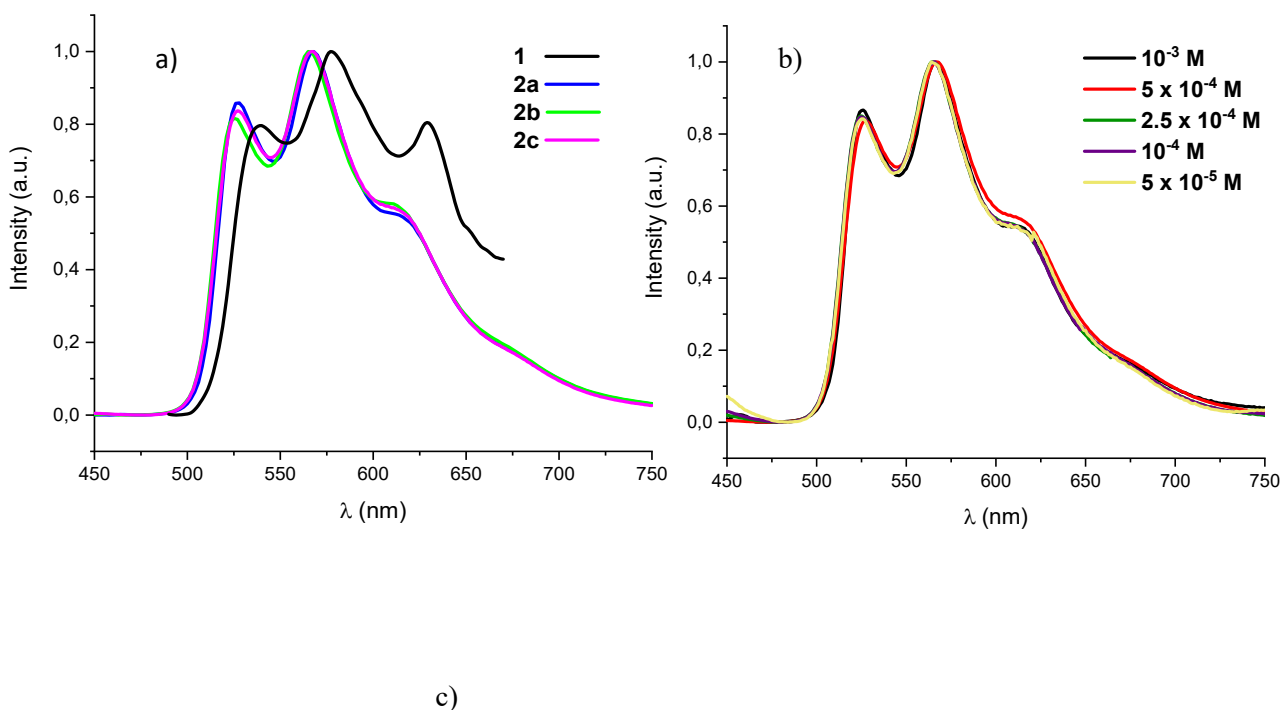
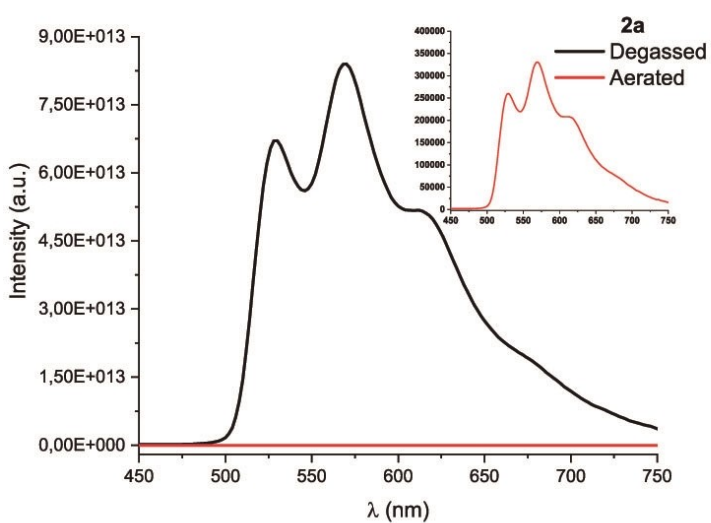
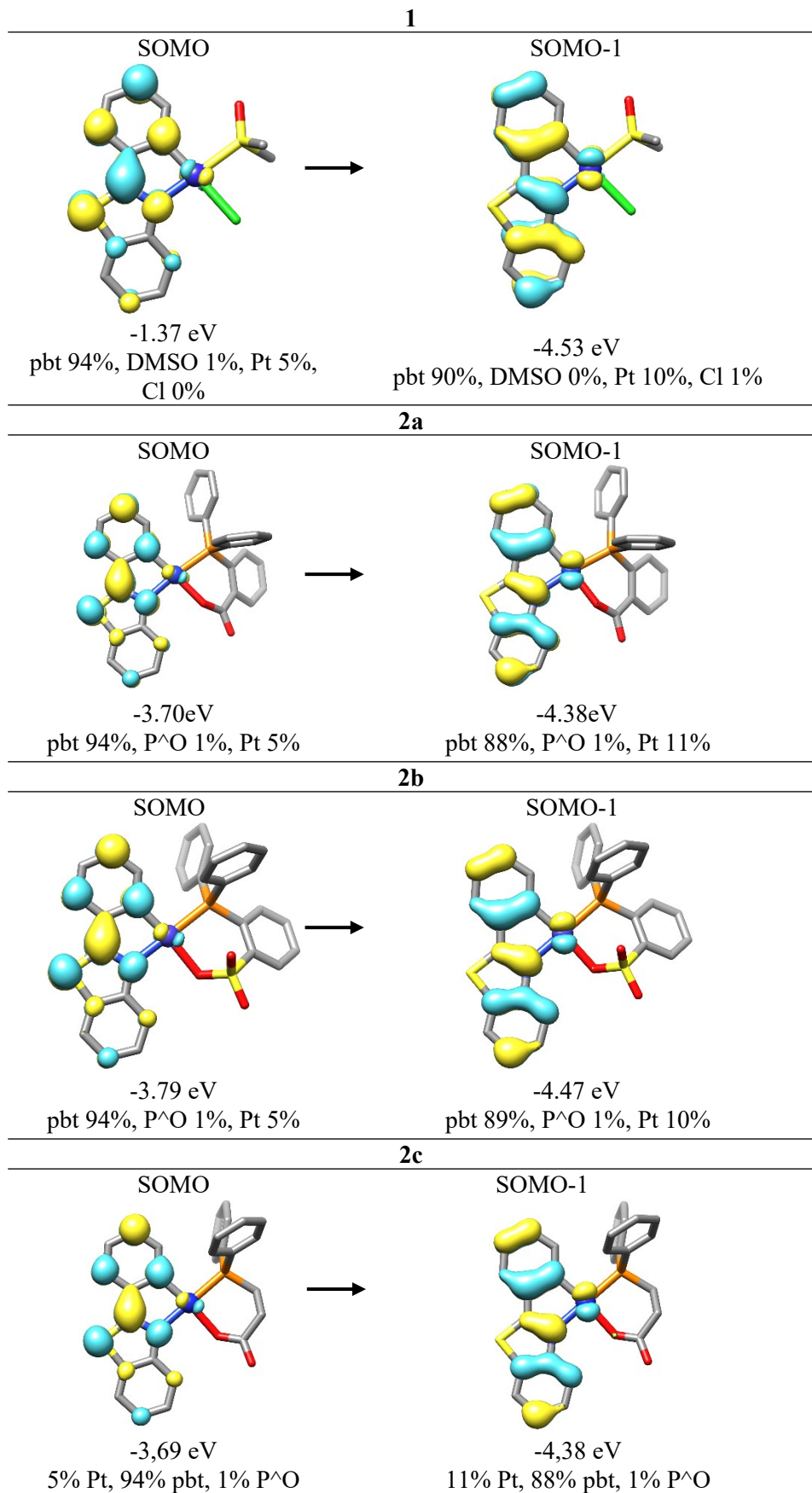


Fig. S15
platinum
degassed
a) at 298 K
b) of **2c** at
298 K, c)
emission
degassed
solution at



Emission spectra of complexes in CH_2Cl_2 5×10^{-4} M (λ_{exc} 400-420 nm), several concentrations at 298 K. Comparison of the spectra of **2a** in degassed and aerated CH_2Cl_2 at 298 K.



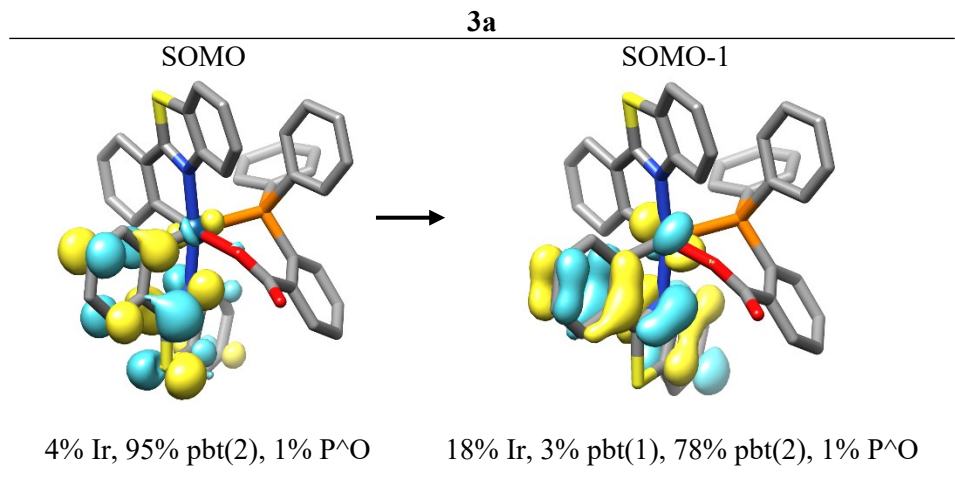


Fig. S16 Plots and composition (%) of the frontier MOs in CH₂Cl₂ of **1**, **2a**, **2b**, **2c** and **3a**

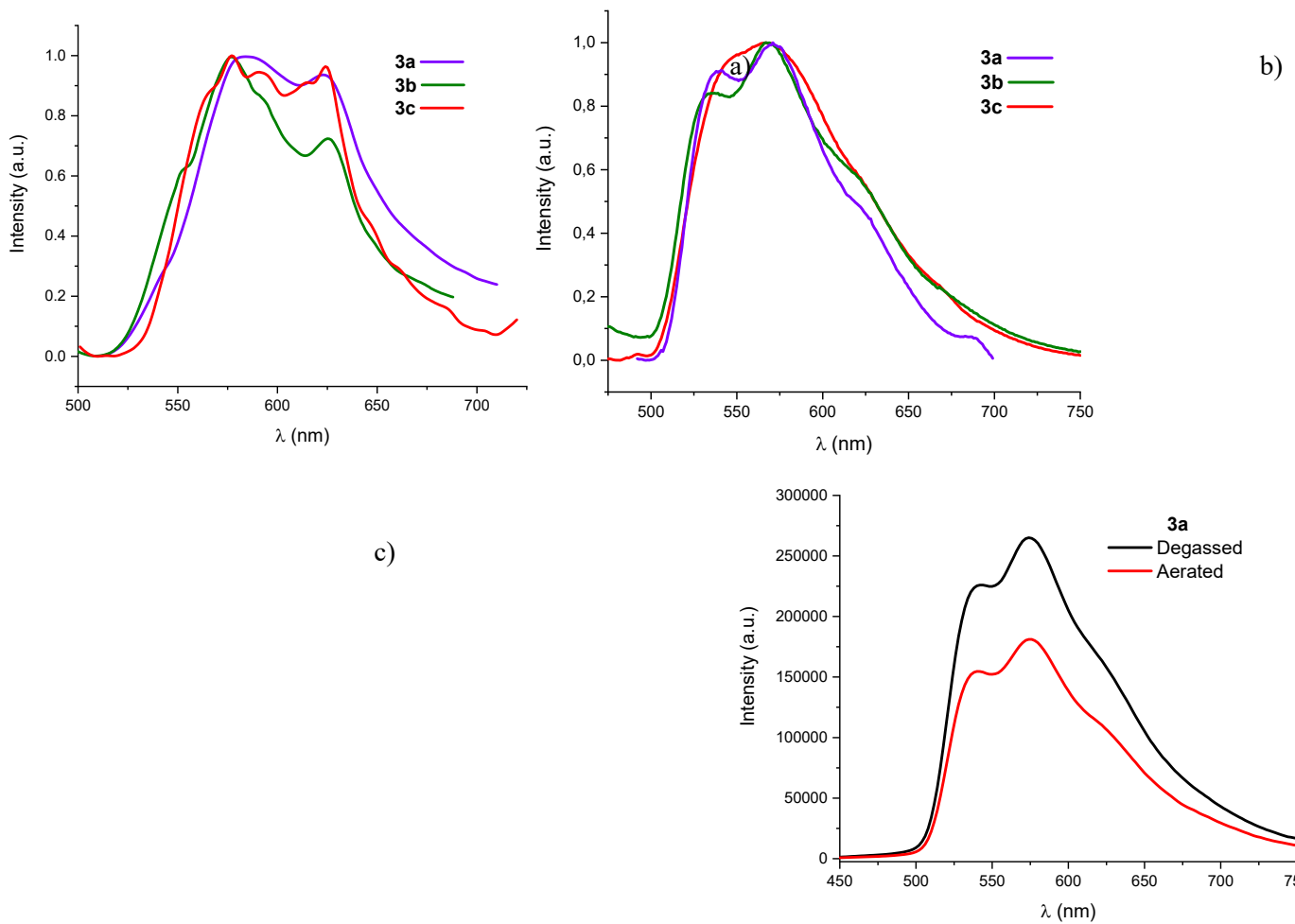


Fig. S17 Emission spectra of iridium complexes a) in solid state at 298 K, b) in degassed CH_2Cl_2 5×10^{-4} M (λ_{exc} 400-420 nm), c) Comparison of the emission spectra of **3a** in degassed and aerated CH_2Cl_2 solution at 298 K.

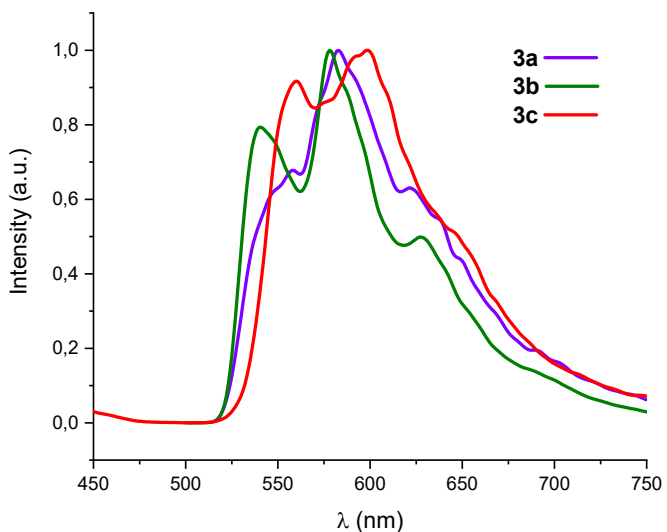


Fig. S18 Emission spectra of iridium complexes in solid state at 77 K.